PCCP

The rotationally resolved electronic spectrum of *p*-cyanophenol

Jochen Küpper,† Michael Schmitt* and Karl Kleinermanns

Heinrich-Heine-Universität, Institut für Physikalische Chemie, 40225, Düsseldorf, Germany. E-mail: mschmitt@uni-duesseldorf.de

Received 11th June 2002, Accepted 9th August 2002
First published as an Advance Article on the web 2nd September 2002

The electronic origin transition of *p*-cyanophenol (4-hydroxy-benzonitrile) at 35547.46 cm^{-1} was examined using rotationally resolved LIF spectroscopy. The experimentally determined inertial parameters are reported and compared to the results of *ab initio* calculations. The S_1-lifetime of *p*-cyanophenol is determined to be 10.6 ± 3 ns, considerably longer than the excited state lifetime of phenol (2.4 ns). This reduction of the rate of internal conversion compared to phenol is explained by different electronic coupling matrix elements for the internal conversion in phenol and *p*-cyanophenol. The barrier to internal rotation of the hydroxy group in the ground states is determined from the observed splitting of the rovibronic lines to 1420 ± 20 cm^{-1}. This barrier is compared to values for the ground and first excited electronic state calculated by *ab initio* theory.

1 Introduction

The increasing acidity of substituted phenols upon electronic excitation raises the question about the structural changes accompanying the transition. The determination of these structural changes is an important tool for the interpretation of excited state proton transfer (ESPT) in complexes of these photoacids. In this publication we want to elucidate the relations between the electronic nature of the substituent and molecular properties. Torsional barriers, bond lengths and angles and acidity in different electronic states are of considerable interest with respect to potential photoacidity. The pK_a value of phenol is known to decrease from 9.82 to 6 upon electronic $S_1 \leftarrow S_0$ excitation. This increase in acidity was contributed to an electron shift from the hydroxy group into the aromatic ring,[1] although more recent theoretical studies point out, that the role of the deprotonated phenolate anion is more important than electronic effects in the protonated species.[2] The pK_a value of *p*-cyanophenol (4-hydroxy-benzonitrile, PCP) has been determined to be 7.74 in the S_0 state and 3.33 in the S_1 state,[3] thus PCP is a stronger acid than phenol in both electronic states. Furthermore the *increase* in acidity upon electronic excitation is larger in PCP. A widely used quantification of the influence of the electronic nature of substituents on the physical properties of aromatic molecules has been given by Hammett.[4,5] Recently, theoretical studies have been performed to connect the pK_a values of different aromatic acids or bases with the nature of an additional substituent in the ring.[6,7] A direct influence of the electronic nature of the substituent in aromatic systems on the torsional frequency of the phenolic hydroxy group has been determined by Fateley *et al.*[8]

The constitution of *p*-cyanophenol (for the atomic numbering of PCP see Fig. 1) can be derived from the structures of phenol and of benzonitrile, which both have been studied extensively by high resolution spectroscopy in the gas phase.

Phenol itself is well studied in the ground and electronically excited state. A full substitution structure of the ground state was derived by Larsen *et al.*[9,10] The electronically excited state was examined by Martinez *et al.*[11] and Berden *et al.*[12] using LIF spectroscopy. Recently a partial substitution structure for the electronically excited state of phenol has been given by our group.[13] The analysis showed an expansion of the aromatic ring upon electronic excitation and an increase of the OH bond length of about 2 pm, reflecting the increased acidity in the S_1-state.

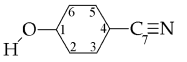

Fig. 1 The structures and atomic numbering of *p*-cyanophenol. Experimental and theoretical geometric parameters for both electronic states are given in Table 2.

The $S_1 \leftarrow S_0$ origin transition of phenol is a superposition of two bands split by 56 MHz,[12] originating from different torsional substates, which are due to the internal rotation of the hydroxy group. The barriers to internal rotation could be determined to be 1215 ± 10 cm^{-1} in the electronic ground state and 4710 ± 30 cm^{-1} in the first electronically excited state. Within the spectral resolution of these experiments phenol has to be described by the molecular symmetry group G_4.

The vibronic ground state of benzonitrile has been studied by microwave spectroscopy,[14,15] and its ground state and first excited electronic state by high resolution laser spectroscopy.[16,17] The molecule has been found to be of C_{2v} symmetry in both electronic states, *i.e.* with a linear C–C≡N minimum configuration. The structure of PCP was calculated at the HF and MP2 levels of theory, and an *ab initio* normal mode analysis was compared to experimental IR frequencies.[18]

Recently, laser induced dispersed fluorescence spectra of PCP and a comparison of experimental vibrational frequencies to *ab initio* calculated normal mode frequencies were reported by Roth *et al.*[19] So far, no high resolution studies of gas phase *p*-cyanophenol have been published. We herein report the results of rotationally resolved laser spectroscopy of the $S_1 \leftarrow S_0$ vibronic origin transition. Although the determination of just one set of rotational constants is of course not sufficient for a complete geometry determination, these data can be used as additional boundary conditions in fits of the Franck–Condon intensity patterns, which is an alternative approach to determine excited-state structures.[20]

† Present address: University of North Carolina, Department of Chemistry, Chapel Hill, NC 27599, USA.

 DOI: 10.1039/b205644e

2 Experimental setup and computational details

The experimental setup for high resolution LIF is described in detail elsewhere.[21] Briefly, it consists of a ring dye laser (Coherent 899-21), which is pumped with 6 W of the 514 nm line of an Ar^+-ion laser (Coherent Innova 100). This light is coupled into an external folded ring cavity (LAS WaveTrain)[22] for second harmonic generation (SHG). Typical UV powers are 2–10 mW. The molecular beam machine consists of three differentially pumped vacuum chambers that are linearly connected by skimmers. The expansion chamber is evacuated by a 8000 l s^{-1} oil diffusion pump (Leybold DI 8000), which is backed by a 250 m^3 h^{-1} roots blower pump (Saskia RPS 250) and a 65 m^3 h^{-1} rotary pump (Leybold D65B). The second chamber serves as buffer chamber and is pumped by a 400 l s^{-1} turbo-molecular pump (Leybold Turbovac 361), backed by a 40 m^3 h^{-1} rotary pump (Leybold D40B), maintaining a chamber pressure below 1×10^{-5} mbar. The third chamber is pumped by a 145 l s^{-1} turbo-molecular pump (Leybold Turbovac 151) through a liquid nitrogen trap and backed by a 16 m^3 h^{-1} rotary pump (Leybold D16B) resulting in a vacuum better than 1×10^{-6} mbar. The molecular beam is crossed at right angles with the laser beam 360 mm downstream of the nozzle. The laser induced fluorescence is collected perpendicular to the plane defined by laser and molecular beam by an imaging optics setup consisting of a concave mirror and two plano-convex lenses.

PCP was purchased from Fluka (>97%). The sample was heated to 200 °C, seeded in Argon and expanded through a 150 μm nozzle at a backing pressure of 600 mbar.

The *ab initio* calculations have been performed using the Gaussian 98 program package.[23] The SCF convergence criterion used for our calculations was an energy change below 10^{-8} E_h, while the convergence criterion for the gradient optimization of the molecular geometry was $\partial E/\partial r < 1.5 \times 10^{-5}$ $E_h a_0^{-1}$ and $\partial E/\partial \varphi < 1.5 \times 10^{-5}$ $E_h/°$, respectively. A normal mode analysis has been performed utilizing the analytical second derivatives of the potential energy surface.

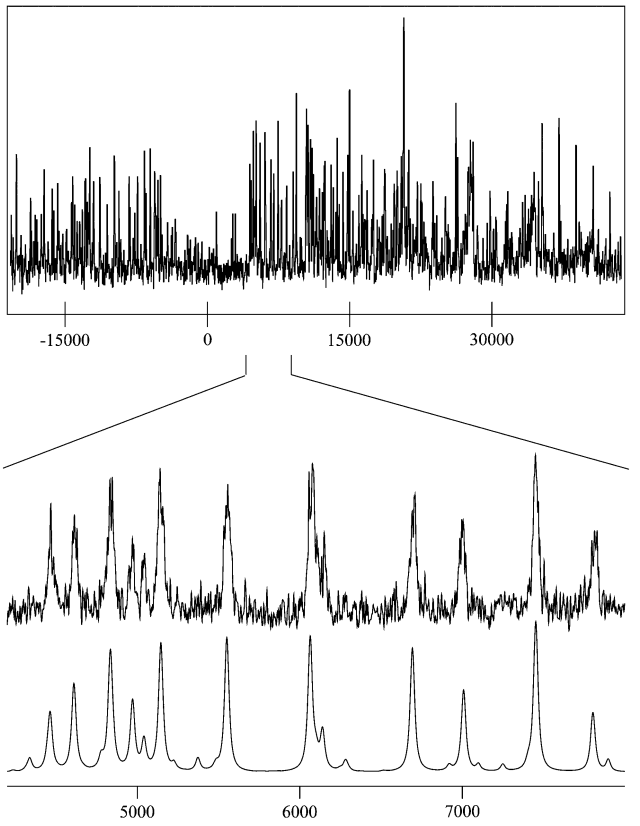

Fig. 2 High resolution electronic spectrum of *p*-cyanophenol. The origin frequency (0 on the figure abscissa) is at 35547.46(1) cm^{-1}. The uppermost trace shows the experimental spectrum, whereas the lower traces show an expanded portion of the experimental trace and the corresponding part of the simulation.

3 Results and discussion

The LIF spectrum of the electronic origin of PCP along with part of the simulation is shown in Fig. 2.

In the high resolution laser induced fluorescence spectrum of the electronic origin of PCP 89 single rovibronic lines are assigned. They are fit by an asymmetric rigid rotor Hamiltonian, using a rotational temperature of 4.0 K, and *b*-type selection rules. PCP is a near prolate symmetric top in the S_0 and S_1 states, with $\kappa_0 = -0.9378$ and $\kappa_1 = -0.9305$, respectively. The molecule is planar in both electronic states, as can be derived from the inertial defects, namely -0.078 u Å^2 in the ground state and -0.274 u Å^2 in the electronically excited state. The experimental inertial parameters are given in Table 1, along with results from *ab initio* calculations performed with the Gaussian 98 program package.[23]

3.1 Determination of the structure

A comparison of the experimentally determined rotational constants for the S_0 and S_1 states with the results of *ab initio* calculations (Table 1) shows very good agreement. The ground state rotational constants are reproduced to within less than 2%, even for SCF calculations with moderate basis sets. The rotational constants of the electronically excited state have been calculated at the CIS/6-311++G(d,p) level with absolute deviations around 1–2%, and at the CAS(10,9)/6-31G(d,p) level with differences of less than 1.5%. Even the changes of the rotational constants upon electronic excitation are in accordance with the changes calculated at the SCF level (HF//CIS).

In order to deduce the structure changes upon electronic excitation from the experimental rotational constants, several assumptions have to be made concerning the model. The determination of a molecular structure from a fit of structural parameters to experimental rotational constants is not straightforward due to the nonlinear relation between the structural parameters and the inertial constants. In a recent publication, we described a computer program, capable of fitting a structure to rotational constants using different molecular models and different structure definitions[13] and its test on the structure of phenol, using a set of rotational constants from twelve different isotopomers.

Helm *et al.*[16] and later Borst *et al.*[17] reported the rotational constants of benzonitrile for the electronically excited state. Both studies relied on ground state rotational constants from MW studies.[14,15] With the slightly more accurate inertial parameters of Borst *et al.*, we calculated a model structure for both electronic states, using our newly developed program *pKrFit*.[13] The obtained structural change of benzonitrile upon electronic excitation will be utilized in the following in order to determine structural changes upon electronic excitation of PCP. The utilization of only two rotational constants (due to the planarity of the system the third constant is linearly dependent on these two), for the determination of a molecule with 33 degrees of freedom, demands a very restricted model, of course. Helm *et al.*[16] set the interatomic distances and angles in the aromatic ring equal to the respective values of benzene. The C–N bond length was set to the value in HCN, whereas the distance of the center of mass (COM) to the C_7-atom was fit.

Table 1 Molecular constants of *p*-cyanophenol in its S_0 and S_1 states from high resolution spectroscopy and *ab initio* calculations.[23] One standard deviation for the experimental values in parentheses are shown in units of last digit. Calculated ground state constants are given for Hartree–Fock and MP2 calculations for 6-311G(d,p) and 6-311++G(d,p) basis sets. Reported changes of the calculated rotational constants upon electronic excitation are obtained from the differences between HF and CIS calculations for these basis sets. CASSCF calculations at the 6-31G(d,p) basis set are given for the ground and excited states. Theoretical transition frequencies are obtained from the HF/CIS and the CASSCF calculations, respectively, and are corrected for vibrational zero-point effects

Parameters	Experiment	HF/6-311G(d,p) and HF//CIS/ 6-311G(d,p)	MP2/6-311G(d,p)	HF/6-311++G(d,p) and HF//CIS/ 6-311++G(d,p)	MP2/ 6-311++G(d,p)	CAS(10/9)/ 6-31G(d,p) (S_0 (S_1)[a]
A''/MHz	5611.7 (1)	5718	5605	5714	5597	5646
B''/MHz	990.1 (1)	1004	982	1004	982	991
C''/MHz	841.7 (1)	854	836	854	835	843
κ''	−0.9378 (1)					
$\Delta I''$/u Å^2	−0.078 (5)					
$A' - A''$ (MHz)	−305.86 (59)	−340		−344		−291
$B' - B''$ (MHz)	0.18 (5)	+3		+5		−15
$C' - C''$ (MHz)	−6.82 (3)	−12		−5		−17
κ'	−0.9305(1)					
$\Delta I'$/u Å^2	−0.274 (7)					
ν_0/cm^{-1}	35547.46(1)	45 829		44 932		36 438

[a] These calculations are from ref. 19.

We use a slightly different model, which is described in the following. All C–C bond lengths in the aromatic ring are set equal and are fit. The C_4–C_7 distance is fit as well, whereas the C_7–N bond length is fixed to 115.6 pm, as determined in a MW study of benzonitrile.[14] The C–H bond lengths in the electronic ground state have been fixed to 108.1 pm, the experimentally determined MW value, and to 107.2 pm in the electronically excited state, reflecting the average bond shortening upon excitation, as found in benzene.[27] All C–C–C angles in the aromatic ring have been set to 120°. Within this model, we obtained for the ground state (excited state) an average C–C bond length in the aromatic ring of 140.148(3) pm (142.80(2) pm) and a C_4–C_7 distance of 141.98(2) pm (143.07(2) pm). Of course, these uncertainties reflect only the propagated uncertainties of the rotational constants, and do not contain errors of the model.

The geometry changes in phenol upon electronic excitation have been determined from the rotational constants of twelve isotopomers.[13] In order to compare the geometry changes in phenol and PCP we will take the r_0-geometry parameters of phenol, which depend considerably on the isotopomer. Nevertheless, due to a lack of sufficient experimental parameters, this is the only value we can get for PCP. Since we use the same isotopically (un)substituted molecules this should not be a problem. In phenol the aromatic ring expands upon electronic excitation. The average C–C bond length in the phenol ring increases from 139.4 to 143.9 pm upon electronic excitation. The C–O bond length decreases from 136.8 to 132.6 pm, whereas the O–H bond length increases from 96.2 to 99.2 pm.

With only one set of rotational constants for the PCP molecule, the model for the geometry to be fit has to be restricted considerably. We employed two different models, which are given in Table 2 and will be defined in the following. These two models present only an arbitrary selection of several models, which all suffer from discrepancies due to the limited number of parameters. The choice of especially these two models is guided by chemical reasoning.

In model I, the mean C–C bond length has been set to the experimentally determined phenol value. The C_4–C_7 and C_7–N distances in both electronic states have been set to the experimental values of benzonitrile. With these starting values, the C–O bond length and the O–H bond length of PCP have been fit in both electronic states. Whereas the C–O bond length decreases from 137.49 to 131.9 pm, the O–H bond expands from 99.3 to 111 pm. Of course, this large increase in O–H bond length is partially an artifact due to the oversimplified model geometry, *e.g.* the assumption of a constant C_7–N distance in the nitrile group upon electronic excitation is a very rough approximation.

Model II is based mainly on the *ab initio* values from ref. 19 which are given in the last column of Table 2 for comparison. Using an average value for all aromatic C–C bond length as in model I did not result in a satisfactory fit of the rotational constants. The only way to obtain a numerically stable fit with a χ^2 comparable to the fit using model I is the assumption of different C–C bond length in the aromatic ring. Therefore we defined two different bond length parameters. One for the bonds C_1–C_2, C_3–C_4, C_4–C_5, C_6–C_1 and one for the bonds C_2–C_3 and C_5–C_6. Using this model, we obtained a fit of equal quality as in model I. The C–C bond lengths in the aromatic ring, which are nearly the same in the electronic ground state, tend to differ considerably upon electronic excitation. The "*para*" bonds are considerably shorter than all other C–C bonds in electronically excited aromatics. This is in contrast to our findings for the excited state structure of phenol,[13] where the experimental results could be explained using an average bond length for the aromatic ring. Thus, it seems, that the model of an quinoidal distortion of the aromatic ring upon electronic excitation is valid for *p*-disubstituted aromatics, as has been shown before by Cvitaš *et al.* and Christoffersen *et al.* but has a limited significance for monosubstituted aromatics.[28–30]

3.2 S_1-state lifetime

Single rovibronic lines in the electronic origin of PCP exhibit lineshapes of split Voigt lines with common Gaussian and Lorentzian contributions to the full width at half maximum of $w_G = 20$ MHz (determined from an analysis of the (unsplit) bands of benzonitrile obtained at the same experimental conditions) and $w_L = 15 \pm 5$ MHz, respectively and a splitting of the two Voigt lines of 20 ± 2 MHz. The splitting, which is due to the internal rotation of the hydroxy group will be handled in the next paragraph. The Lorentzian linewidth, the frequency of the lower energy band, the splitting of the two subbands, the total area, and the baseline have been fit simultaneously to the experimental lineshape of ten rovibronic lines, using the Levenberg–Marquardt algorithm.[31,32] In these fits spin statistical weights of 10 : 6 or 6 : 10, respectively (*cf.* next paragraph), and the Gaussian linewidth were fixed. The lineshape

Table 2 Experimental r_0 geometry parameters and *ab initio* calculated r_e geometry parameters of benzonitrile, phenol and PCP. The experimental parameters are obtained from a fit of the geometry to the experimental inertial parameters. See text for details concerning the different models. MP2 and CIS results are given for the 6-311++G(d,p) basis, CASSCF calculations for the 6-31G(d,p) basis set

					PCP							
	Benzonitrile		Phenol		(Model I)		(model II)		MP2	CIS	CASSCF[19]	
	S_0	S_1	S_0	S_1	S_0	S_1	S_0	S_1	S_0	S_1	S_0	S_1
$\langle C_{ar}C_{ar}\rangle$[a]	140.1	142.8	139.4	143.9	139.4	143.9	—	—	140.0	141.3	139.6	143.2
C_1C_2	—	—	—	—	—	—	140.1	144.5	140.0	139.9	139.6	142.4
C_2C_3	—	—	—	—	—	—	139.4	137.5	139.5	138.0	139.1	143.1
C_4C_7	142.0	143.1	—	—	142.0	143.1	144.3	142.3	143.4	140.0	144.3	142.3
C_7N	115.6	115.6	—	—	115.6	115.6	114.6	115.1	117.7	114.7	114.6	115.1
C_1O	—	—	136.8	132.6	137.5	131.9	135.0	134.8	136.1	133.1	135.0	134.8
OH	—	—	96.2	99.2	99.3	111.0	94.3	97.0	96.2	94.3	94.3	94.3
$C_{ar}H$	108.1	107.2	107.9	107.1	108.1	107.2	107.5	107.2	108.6	107.3	107.5	107.2
$C_{ar}C_{ar}C_{ar}$	120	120	120	120	120	120	120	120				
$C_{ar}C_{ar}H$	120	120	120	120	120	120	120	120				
$C_3C_4C_7$	120	120	—	—	120	120	120	120				
C_4C_7N	180	180	—	—	180	180	180	180				
C_2C_1O	—	—	123.2	119.8	120	120	120	120				
C_1OH	—	—	107.8	107.5	107	107	107	107				
$\langle$obs − calc$\rangle$[b]	—	—	—	—	0.04	0.19	0.04	0.19				
χ^2	—	—	—	—	0.52	58.3	0.52	58.3				

[a] Average C–C bond length in the aromatic ring. [b] Average experimental − calculated rotational constants in MHz.

fits of two selected transitions are shown in Fig. 3. The central part of the spectrum was taken with a very low scan speed and a high sampling rate in order to improve the signal to noise ratio for the lineshape fit. In these scans the absolute frequency is not well determined and these data cannot be used for the evaluation of the inertial constants.

Averaging the obtained Lorentzian linewidths yields an excited state lifetime of 10.6 ± 3 ns. This is considerably longer than the lifetime of bare phenol (2.4 ns), but shorter than the fluorescence lifetime of benzonitrile of 20 ns.[17] It suggests that the determining factor for the lifetime of PCP is the presence of the phenolic OH group. The short excited state lifetime of phenol was attributed to a rapid internal conversion (IC), with the ground state OH stretching vibration as promoter mode.[24] The first quantum of the OH-stretching mode in phenol is observed at 3656 cm^{-1}.[25] The first, second, and third overtones are found at 7143, 10461, and 13612 cm^{-1}, respectively.[26] For PCP the ν_{OH} stretching vibration was observed at a lower frequency of 3580 cm^{-1}.[18] For phenol a linear interpolation of the frequencies of the vibrational overtones to the electronic excitation energy leads to the conclusion, that at least ten quanta of the stretching vibration are needed to match the vibrationless S_1 state. The OH-stretching vibrational frequency in PCP is only 76 cm^{-1} lower in energy. Therefore, at the energy of the vibrationless S_1 the difference amounts to less than 1000 cm^{-1}. Thus, in phenol and PCP the same number of quanta of the promoter mode is needed to match the energy of the electronic origin. Assuming the same density of states for the (dark) acceptor modes, the only reason for different lifetimes in phenol and PCP must be the different electronic coupling matrix element for the IC.

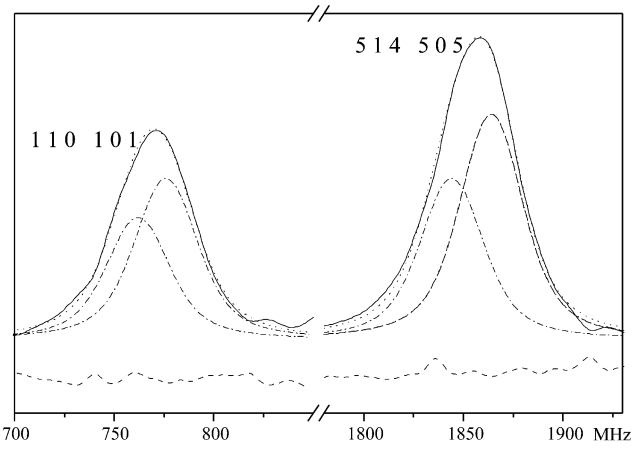

Fig. 3 Lineshape fits of two selected rovibronic lines in the electronic origin of PCP. The dotted traces show the results of a fit of two Voigt profiles to the lineshape of the transitions, the dash dotted lines show the individual Voigt profiles. The lowest trace gives the residues of the fit. For details see text.

3.3 Barriers to internal rotation

The barrier to internal rotation of the hydroxy group can be utilized as a probe of the electronic properties of the aromatic compound. The experimentally determined torsional barrier of phenol amounts to 1215 ± 10 cm^{-1} in the electronic ground state and to 4710 ± 30 cm^{-1} in the electronically excited S_1 state.[12] The lineshape of all rovibronic lines in PCP are unsymmetric due to an unresolved splitting from the internal rotation of the hydroxy group, like in phenol. The fit of the lineshape of ten individual line-doublets resulted in a value for the splitting of 20 ± 2 MHz. In the lineshape fit, the spin statistical weights were fixed to the theoretical value of 10 : 6 for K_a even : odd of the $\sigma = 0$ subtorsional component and to 6 : 10 for the $\sigma = 1$ subtorsional component. The Doppler width was fixed at 20 MHz, *vide supra*.

To determine the barrier to internal rotation we assume that the excited state does not contribute to the line-splitting. This is justified because the torsional barrier in the excited state should be on the order 5000 cm^{-1} by comparison with phenol, leading to a splitting of the subtorsional states of 1.8×10^{-9} cm^{-1} (53 Hz) with a value of the torsional constant F of 690 GHz as determined for phenol.[12] This value is reasonable here since the geometry of the hydroxy group does not change considerably upon substitution in *para*-position. Thus from an observed line splitting of 20 ± 2 MHz a ground state barrier of 1420 ± 20 cm^{-1} can be calculated, 17% higher than for phenol. Using this barrier the $v = 1 \leftarrow v = 0$ torsional transition is calculated to be 339 cm^{-1}. Binev[18] reports an experimental

Table 3 Experimental and calculated barriers to internal rotation of PCP and phenol. All values are given in cm^{-1}

		PCP		phenol	
State	Method	$V_{2,e}$	$V_{2,0}$	$V_{2,e}$	$V_{2,0}$
S_0	Experiment	1420		1215	
	HF/cc-pVTZ	1236	1012	947	764
	HF/6-311G(d,p)	1122	921	897	717
	HF/6-311++G(d,p)	1127	931	846	691
	HF/6-311++G(3df,2pd)	1206	989	917	740
	MP2/6-311G(d,p)	1353	1181	1171	1034
	MP2/6-311++G(d,p)	1205	1080	1033	965
S_1	Experiment	∞[a]		4710	
	CIS/6-311G(d,p)	2093	2230		
	CIS/6-311++G(d,p)	2140	2248	2354	2186

[a] Assumed in the determination of the ground state value. See text for details.

value of 295 cm^{-1}, obtained from a solid sample of PCP in CsI. The torsional frequency of PCP in a cyclohexane solution is reported to be 343 cm^{-1},[8] in very good agreement with the value predicted from our torsional splitting. Indeed, torsional frequencies of para substituted phenols are known to differ only slightly between gas phase and unpolar solutions.[8]

Table 3 gives the experimentally determined barrier to internal rotation together with the *ab initio* calculated barrier heights of phenol and PCP. The ground state barrier of phenol is underestimated by 21% at the MP2/6-311++G(d,p) level. Nevertheless the comparison of the calculated barriers at this level of theory shows a higher ground state barrier for PCP than for phenol of about 21%. The calculated values, at the CIS level, for the excited state barrier of phenol are too small compared to experiment. Nevertheless they show a considerable increase of the barrier to internal rotation upon electronic excitation in phenol. The calculated barriers for PCP are very similar, confirming the assumption of a high barrier in the excited state of PCP used above.

If we assume that valence-bond structures as shown in Fig. 4 represent an important contribution to the reasons for the torsional barrier in phenol, the increased barrier in PCP can be explained by a additional delocalization of the partial negative charge. Because the conjugation between the oxygen lone pairs and the aromatic ring is weaker for the torsional transition state than for the ground state, the stabilization of the transition state is smaller than in the ground state. Additional resonance structures for PCP compared to phenol explain the higher torsional barrier. Equally, this mesomeric effect also stabilizes the *p*-cyanophenolate anion and is the reason for the increased acidity.

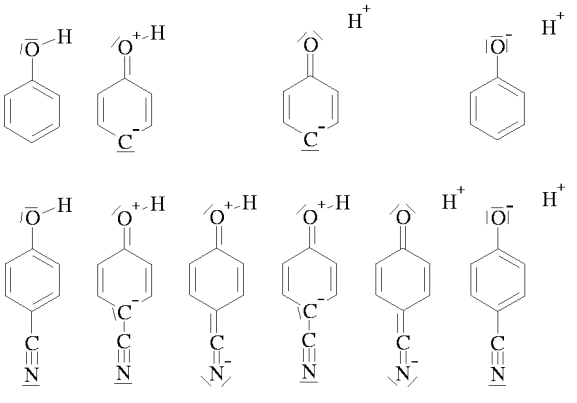

Fig. 4 Valence bond structures of phenol and PCP.

Conclusions

The analysis of the rovibronic spectrum of PCP yields rotational constants for both electronic states, which allow us to obtain structural parameters for both states and to examine changes upon electronic excitation. Within the model employed, we found an increase of the O–H bond length. This O–H bond stretching is accompanied by a decrease of the C–O bond length, as found in phenol. From our analysis of the inertial parameters, the O–H distance of PCP in comparison to phenol was found to be increased in both electronic states, although our restricted geometry model imposes caution in the interpretation of such small effects. Nevertheless, these OH bond lengths comparisons agree with the increased acidity of PCP compared to phenol and the larger increase of acidity upon excitation. The aromatic ring appears to expand in a quinoidal manner upon electronic excitation, due to the electronic effects of the two para substituents.

The barrier to internal rotation of the hydroxy group was determined to be 1420 cm^{-1} in the S_0 state, which is about 17% higher than the corresponding value in phenol. Both, the structural changes, as well as the experimental and theoretical barriers to internal rotation in the S_0 and S_1-state are in agreement with the increased acidity in both electronic states. High resolution electronic spectroscopy can thus be utilized to investigate electronic effects of substituents on different molecular properties. Investigation of a series of appropriate molecules as underway in our laboratory should allow to quantify relations between the properties of functional groups, like bond length, bond strength, torsional barriers *etc.*, and molecular properties of the overall molecule, like acidity *etc.*

Acknowledgements

Petra Imhof and Wolfgang Roth performed some of the *ab initio* calculations. We thank Christian Ratzer for experimental assistance. This work was supported by the Deutsche Forschungsgemeinschaft SCHM1043/9-2.

References

1 L. Salem, *Electrons in Chemical Reactions*, Wiley, New York, 1982.
2 G. Granucci, J. Hynes, P. Millié and T.-H. Tran-Thi, *J. Am. Chem. Soc.*, 2000, **122**, 12 243.
3 S. Schulman, W. Vincent and W. Underberg, *J. Phys. Chem.*, 1981, **85**, 4068.
4 L. P. Hammett, *J. Am. Chem. Soc.*, 1937, **59**, 96.
5 L. P. Hammett, *Trans. Faraday Soc.*, 1938, **34**, 156.
6 K. C. Gross and P. G. Seybold, *Int. J. Quantum Chem.*, 2000, **80**, 1107.
7 K. C. Gross and P. G. Seybold, *Int. J. Quantum Chem.*, 2001, **85**, 569.
8 W. Fateley, G. Carlson and F. Bentley, *J. Phys. Chem.*, 1975, **79**, 199.
9 T. Pedersen, N. W. Larsen and L. Nygaard, *J. Mol. Struct.*, 1969, **4**, 59.
10 N. W. Larsen, *J. Mol. Struct.*, 1979, **51**, 175.
11 S. J. Martinez, J. C. Alfano and D. H. Levy, *J. Mol. Spectrosc.*, 1992, **152**, 81.
12 G. Berden, W. L. Meerts, M. Schmitt and K. Kleinermanns, *J. Chem. Phys.*, 1996, **104**, 972.
13 C. Ratzer, J. Küpper, D. Spangenberg and M. Schmitt, *Chem. Phys.*, 2002, accepted for publication.
14 U. Dahmen, W. Stahl and H. Dreizler, *Ber. Bunsen-Ges. Phys. Chem.*, 1994, **98**, 970.
15 J. Casado, L. Nygaard and G. O. Sørensen, *J. Mol. Struct.*, 1971, **8**, 211.
16 R. M. Helm, H.-P. Vogel and H. J. Neusser, *Chem. Phys. Lett.*, 1997, **270**, 285.
17 D. R. Borst, T. M. Korter and D. W. Pratt, *Chem. Phys. Lett.*, 2001, **305**, 485.
18 Y. I. Binev, *J. Mol. Struct.*, 2001, **535**, 93.

19 W. Roth, P. Imhof and K. Kleinermanns, *Phys. Chem. Chem. Phys.*, 2001, **3**, 1806.
20 S. Schumm, M. Gerhards and K. Kleinermanns, *J. Phys. Chem. A*, 2000, **104**, 10 648.
21 M. Schmitt, J. Küpper, D. Spangenberg and A. Westphal, *Chem. Phys.*, 2000, **254**, 349.
22 M. Okruss, R. Müller and A. Hese, *J. Mol. Spectrosc.*, 1999, **193**, 293.
23 M. J. Frisch, G. W. Trucks, H. B. Schlegel, G. E. Scuseria, M. A. Robb, J. R. Cheeseman, V. G. Zakrzewski, J. A. Montgomery, Jr., R. E. Stratmann, J. C. Burant, S. Dapprich, J. M. Millam, A. D. Daniels, K. N. Kudin, M. C. Strain, O. Farkas, J. Tomasi, V. Barone, M. Cossi, R. Cammi, B. Mennucci, C. Pomelli, C. Adamo, S. Clifford, J. Ochterski, G. A. Petersson, P. Y. Ayala, Q. Cui, K. Morokuma, D. K. Malick, A. D. Rabuck, K. Raghavachari, J. B. Foresman, J. Cioslowski, J. V. Ortiz, A. G. Baboul, B. B. Stefanov, G. Liu, A. Liashenko, P. Piskorz, I. Komaromi, R. Gomperts, R. L. Martin, D. J. Fox, T. Keith, M. A. Al-Laham, C. Y. Peng, A. Nanayakkara, C. Gonzalez, M. Challacombe, P. Gill, M. W. Johnson, W. Chen, M. W. Wong, J. L. Andres, M. Head-Gordon, E. S. Replogle and J. A. Pople, *Gaussian 98, Revision A.7*, Gaussian, Inc., Pittsburgh, PA, 1998.
24 R. J. Lipert and S. D. Colson, *J. Phys. Chem.*, 1989, **93**, 135.
25 H. D. Bist, J. C. D. Brand and D. R. Williams, *J. Mol. Spectrosc.*, 1966, **21**, 76.
26 S. Ishiuchi, H. Shitomi, K. Takazawa and M. Fujii, *Chem. Phys. Lett.*, 1998, **283**, 243.
27 J. Callomon, T. Dunn and I. Mills, *Philos. Trans. R. Soc. London, Ser. A.*, 1966, **259**, 499.
28 T. Cvitaš, J. Hollas and G. Kirby, *Mol. Phys.*, 1970, **19**, 305.
29 J. Christoffersen, J. M. Hollas and G. H. Kirby, *Proc. R. Soc. London, Ser. A.*, 1968, **307**, 97.
30 J. Christoffersen, J. M. Hollas and G. H. Kirby, *Mol. Phys.*, 1970, **18**, 451.
31 K. Levenberg, *Q. Appl. Math.*, 1944, **2**, 164.
32 D. D. Marquardt, *J. Soc. Ind. Appl. Math.*, 1963, **11**, 431.